

## Supplementary Information for

Hard Templating Ultrathin Polycrystalline Hematite Nanosheets and the Effect of Nano-dimension on CO<sub>2</sub> to CO Conversion via the Reverse Water Shift Reaction

Zachary S. Fishman,<sup>a</sup> Yulian He,<sup>a</sup> Ke R. Yang,<sup>b</sup> Amanda Lounsbury,<sup>a</sup> Junqing Zhu,<sup>c</sup> Thanh Minh Tran,<sup>a</sup> Julie B. Zimmerman,<sup>a</sup> Victor S. Batista,<sup>b,\*</sup> Lisa D. Pfefferle<sup>a,\*</sup>

<b>Synthesis of Iron Hydroxide Nanostructures.....</b>	<b>2</b>
<b>Polycrystallinity of Hematite Nanosheets.....</b>	<b>3</b>
<b>Temperature Sensitivity of Goethite Nanowire Synthesis.....</b>	<b>4</b>
<b>Quantification of Nanosheet Thickness.....</b>	<b>5</b>
<b>Derivation of Nanowire Diameter from Surface Area.....</b>	<b>6</b>
<b>FTIR Spectroscopy of Iron Oxide and Hydroxide Nanostructures.....</b>	<b>7</b>
<b>Peak Deconvolution of XPS Spectra.....</b>	<b>8</b>
<b>RWGS-TPR Turn Over Frequency plots of Iron Oxide Nanomaterials.....</b>	<b>9</b>
<b>Complete Mass Spectrum Data for Selectivity.....</b>	<b>10</b>
<b>Composition Change of Iron Oxide Nanosheets Heated in H<sub>2</sub>.....</b>	<b>11</b>
<b>Stability of Iron Oxide Nanosheets.....</b>	<b>12</b>

### Synthesis of Iron Hydroxide Nanostructures

Iron hydroxide nanowires and nanosheets were synthesized and imaged in figure S1 using SEM (a, b) and TEM (b-f). In e and f, EDX mapping was used on TEM-HAADF images of iron hydroxide nanosheets before the copper oxide was removed via ammonium hydroxide washing. Though there is significant overlap due to wrapping, the iron hydroxide nanosheets are clearly distinguishable from the copper oxide nanosheet regions.

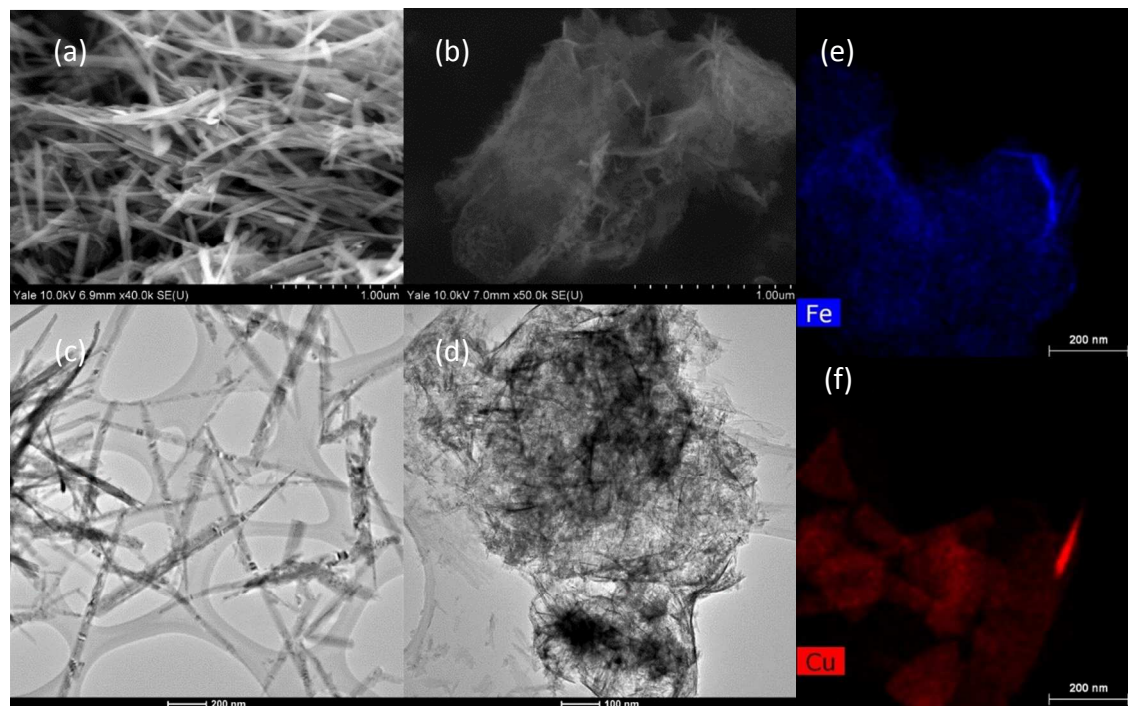


Figure S1. SEM (a,b) and TEM (c,d) of goethite nanowires (a,c) and 6 line ferrihydrite nanosheets (b,d). Energy Dispersive X-ray mapping was used to clearly identify the regions of the sample in figure 2 that contained iron (e) and copper (f). TEM samples were prepared on a gold grid to minimize the effect of background copper signal.

### Polycrystallinity of Hematite Nanosheets

Additional evidence for the polycrystallinity of these hematite nanosheets was found using TEM images as well as diffraction patterns from SAED. In Figure S2 we see a zoomed in image taken of a single hematite nanosheets, a, and it's corresponding SAED pattern, b.

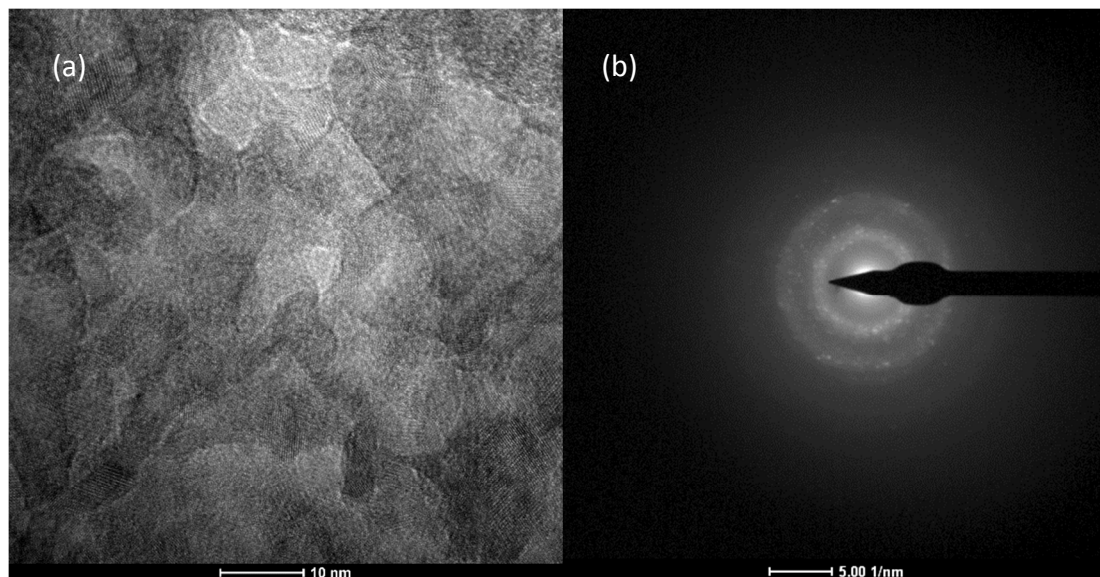


Figure S2. Zoomed in TEM image of a hematite nanosheets (a), and SAED pattern (b) taken at the same location.

### Temperature Sensitivity of Goethite Nanowire Synthesis

In a typical synthesis of goethite nanowires the temperature is kept at 50°C, Figure S3 a. Increasing the temperature of this reaction to 55°C, Figure S3 b, or 60°C, Figure S3 c, results in the formation of nanoparticles alongside the nanowires.

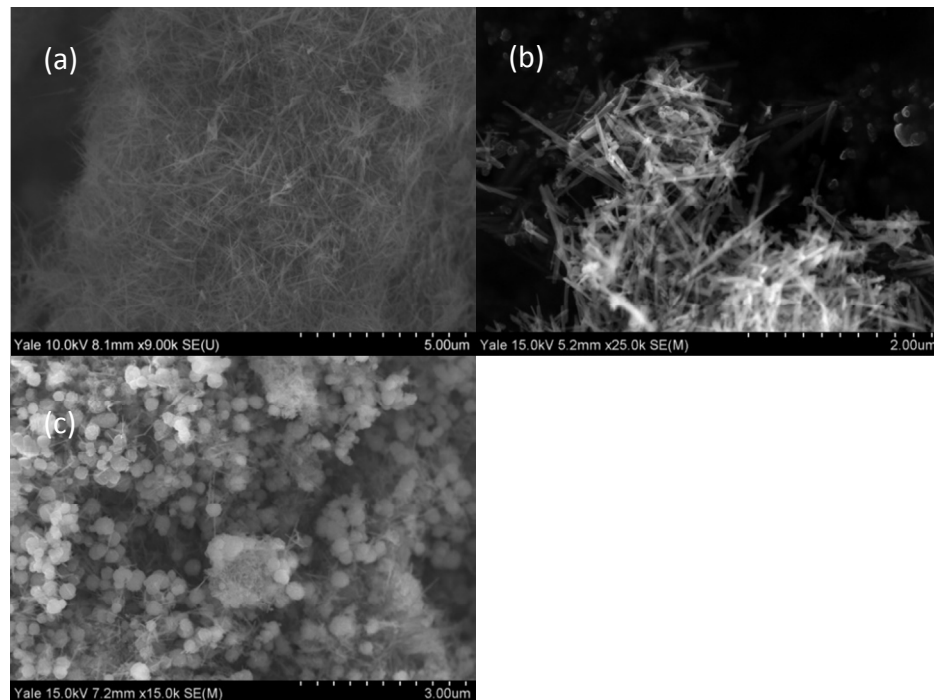


Figure S3. SEM images of goethite nanowires synthesized at different temperatures. In a standard synthesis (a) the temperature was held at 50°C producing well-structured nanowires. When the temperature is elevated to 55°C (b) and to 60°C (c) nanoparticles start to form in addition to the nanowires.

### Quantification of Nanosheet Thickness

Atomic force microscopy was used to quantify iron oxide nanosheet thickness, figure S3 a, and corroborate TEM diameter measurements of iron oxide nanowires, figure S4 b. Here, the nanosheets were found to have a thickness ranging from 4-7 nm while the nanowires had a diameter of 20nm. Height measurements scanning over the nanosheets revealed a steep edge step as well as a large amount of surface roughness while the nanowires appear to be smoother.

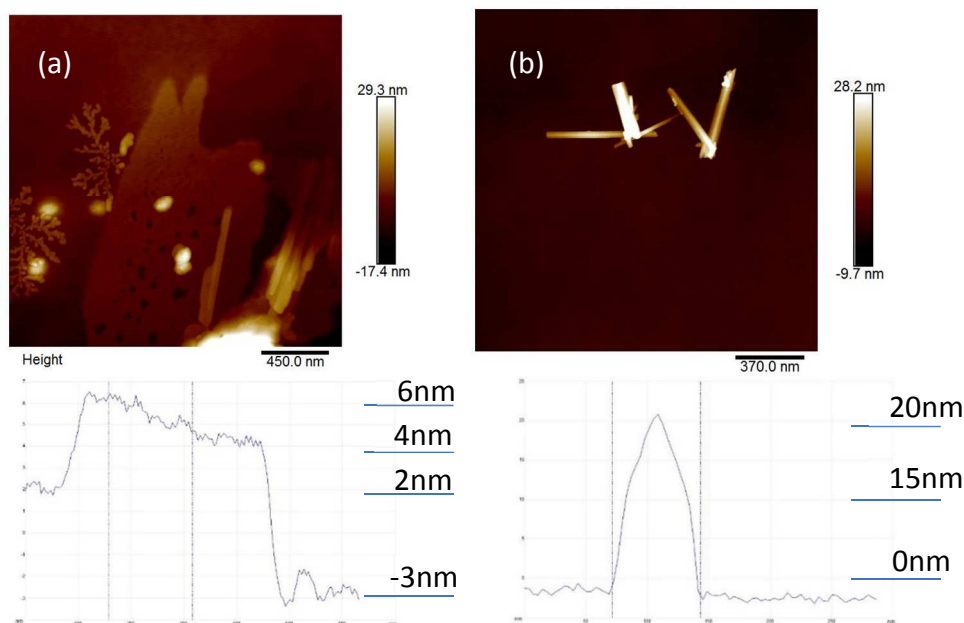


Figure S4. AFM images of Hematite nanosheets (a) and hematite nanowires (b). The nanosheets were found to range in thickness from 4-7 nm. The thickness of the nanowires were found to be 20 nm, consistent with SEM and TEM observations.

### Derivation of Nanowire Diameter from Surface Area

Geometrically nanowires can be approximated as closed cylinders with radius,  $r$ , and length,  $h$ .

$$\begin{aligned} \text{Volume (V) of a Cylinder} &= \pi r^2 h \\ \text{Surface Area (SA) of a Cylinder} &\cong 2\pi r h \end{aligned}$$

Taking the ratio of Volume to surface area we find,

$$\frac{V}{SA} = \frac{r}{2}$$

It is difficult to measure volume and surface area directly, however it is straightforward to measure the surface area of a sample per unit mass, SSA. Additionally, the volume per unit mass of a material is simply the inverse of the density,  $\rho$ . The equation then becomes,

$$\frac{2}{\rho \times SSA} = r, \text{ or } \frac{4}{\rho \times SSA} = d$$

Where  $d$  is the diameter of the nanowire.

Equations for Nanosheets and Nanoparticles

$$\text{Nanosheets: } \frac{2}{\rho \times SSA} = t$$

$$\text{Nanoparticles: } \frac{6}{\rho \times SSA} = d$$

Where  $t$  is nanosheet thickness and  $d$  is nanoparticle diameter

### ATR-FTIR Spectroscopy of Iron Oxide and Hydroxide Nanostructures

In order to glean further insights into the composition of iron oxide and hydroxide nanomaterials ATR-FTIR was performed. In figure S6 we find that ATR-FTIR spectra of the hematite nanomaterials are very similar and the slight variations are discussed in the main body of the manuscript. The goethite nanowires display many peaks making it simple to identify it, while the 6-line ferrihydrite contains few features making other characterization techniques such as XPS necessary to understand its chemical structure.

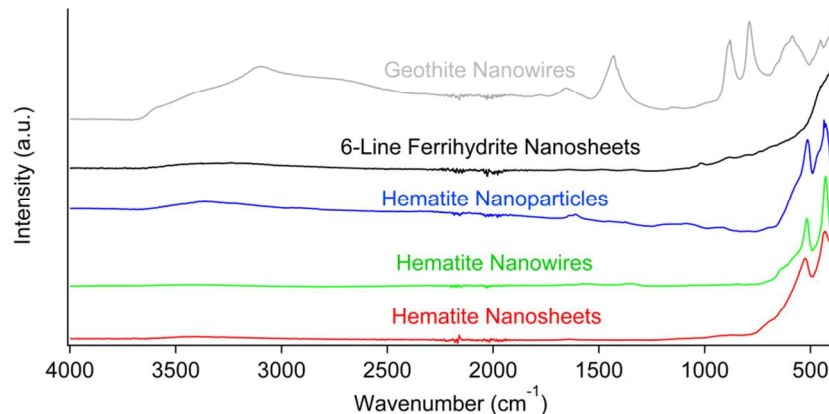


Figure S5. ATR-FTIR spectra of iron oxide and hydroxide nanostructures. The noise from approximately 1900-2300cm<sup>-1</sup> in each sample is attributed to a known defect in the sapphire crystal present in the instrument.

Peak Deconvolution of XPS Spectra

6-Line ferrihydrite nanosheets, goethite nanowires, and hematite nanoparticles all showed multiple peaks at the O 1s edge in XPS. Here, the peaks have been deconvoluted for each sample and a table with the information regarding the peaks has been provided, as shown below in Figure S6.

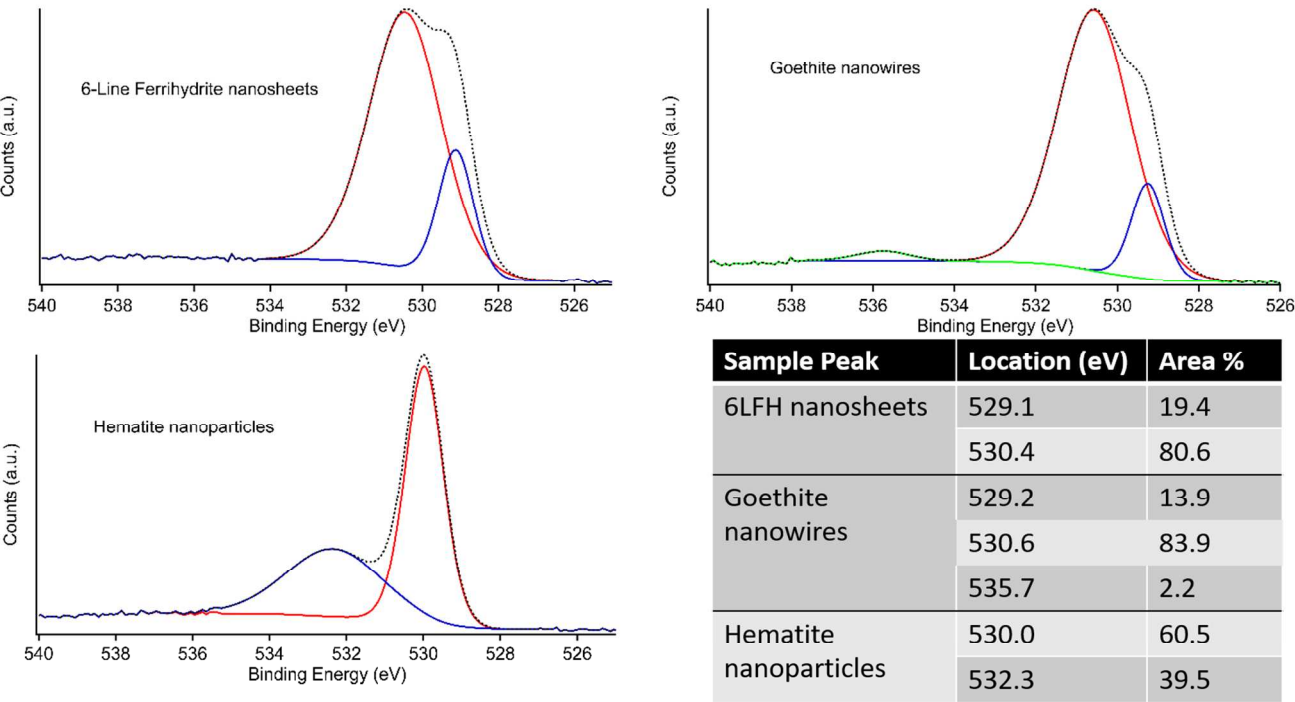


Figure S6- XPS O 1s spectra of selected samples 6-Line Ferrihydrite (6LFH), Goethite nanowires, and Hematite nanoparticles, from Figure 4. These samples had multiple oxygen species and so the peaks associated with each species have been deconvoluted and their parameters given in the accompanying table.



### Complete Mass Spectrum Data for Selectivity

Reverse Water Gas Shift (RWGS)-Temperature Programmed Reaction (TPR) was performed on iron oxide nanosheets, nanowires, and nanoparticles and their associated complete mass spectrum results are shown below, Figure S8. The right column displays the “zoomed in” portion of graphs on the left in order to enhance visibility. The SRS RGA 100 mass spectrometer, used here, acquires data every 3 seconds on up to 10 separate mass to charge ( $m/z$ ) channels. Argon, measured using  $m/z=40$ , was used as an inert carrier gas and its signal intensity remained relatively constant for the duration of the experiment. No other products besides CO and H<sub>2</sub>O were detected.

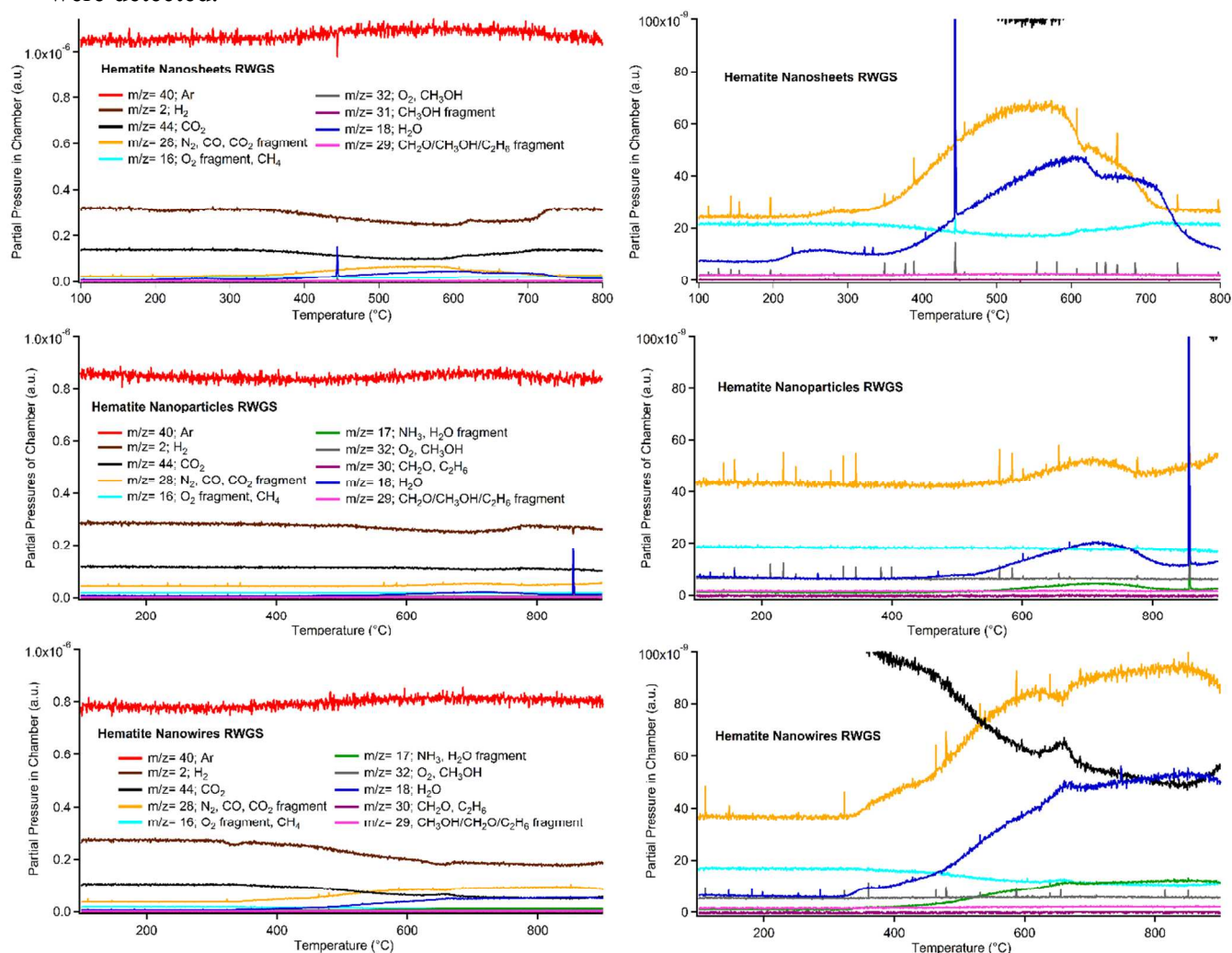


Figure S7. Partial pressure of each species listed is plotted as a function of temperature as by the mass spectrometer during RWGS-TPR for hematite nanosheets (a), nanowires (b), and nanoparticles (c). In this mode data can be collected every 3 seconds from up to 10  $m/z$  channels. The  $m/z$  channels are listed on the figure and color coded for each run. Species that appear at that  $m/z$  are listed for convenience; note that this is not an exhaustive list.

### RWGS-TPR Turn Over Frequency plots of Iron Oxide Nanomaterials

In order to accurately compare the sites of the various iron oxide nanomaterials mass spectrometry data on  $\text{CO}_2$  conversion was normalized to the surface area of each respective nanomaterials, figure S7. On a per site basis we find the nanowires reign supreme at all temperatures measured. The noise in the nanoparticles plot is associated caused by their relatively low surface area making it necessary to plot them on a separate graph.

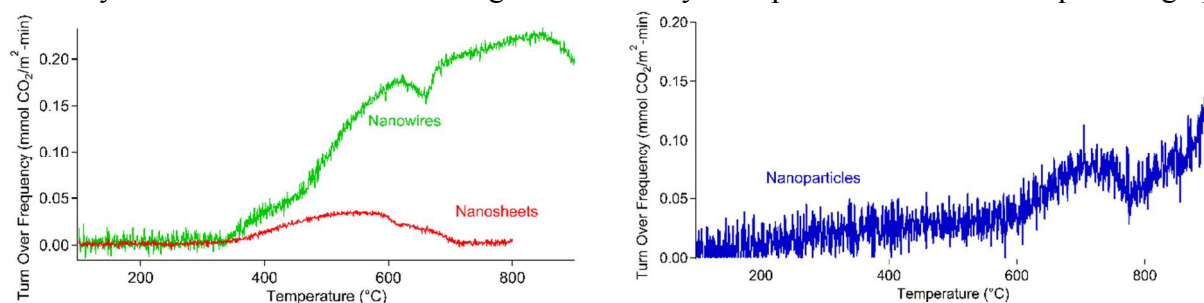


Figure S8. TOF for hematite nanoparticles, nanosheets and nanowires computed using mass spectrometry data during RWGS-TPR and BET surface area measurements.

### Composition change of Iron Oxide Nanosheets Heated in H<sub>2</sub>

XRD was performed on iron oxide nanosheets removed at different temperatures during the H<sub>2</sub>-TPR process, Figure S9 a. We find a transition in crystal structure from hematite to magnetite at 250°C and then to iron metal from 500°C to 700°C. The SEM image, b, is taken of an iron oxide nanosheet sample after TPR at 250°C. We see that the structure is highly defective, however the overall nanosheet shape is conserved despite the change in composition

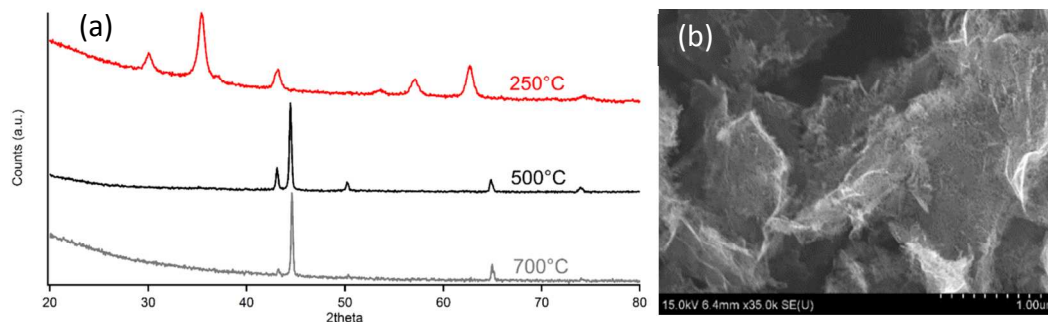


Figure S9. XRD spectra of hematite nanosheets after TPR at 250, 500, and 700°C, (a), and an SEM image of the nanosheets after TPR at 250°C (b).

### Stability of Iron Oxide Nanosheets

SEM images of iron oxide nanosheets and nanowires were acquired after 15 minutes of RWGS reaction at 500°C, figure S10 a, b. While it seems that the nanowires are better able to maintain their structure than the nanosheets, we observe morphology changes in both. XRD spectra taken of the nanosheets after this process, c, reveals that they have indeed converted to magnetite.

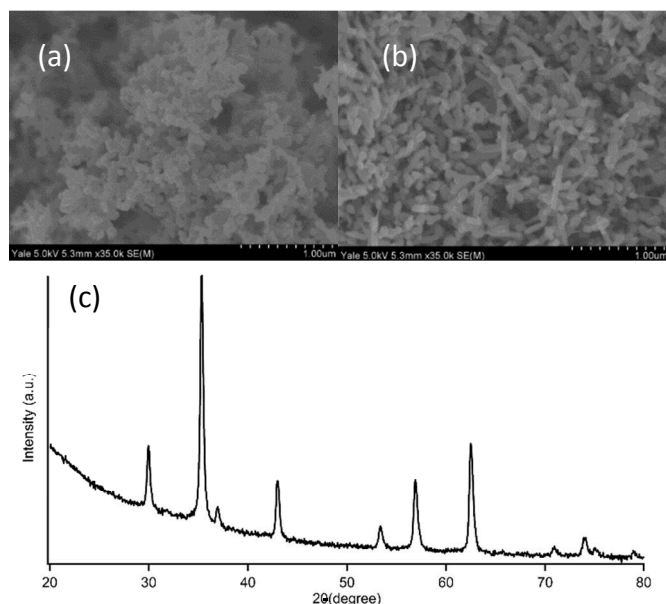


Figure S10. SEM images of hematite nanosheets (a) and nanorods (b) after 15 minutes of RWGS reaction at 500°C. (c) shows an XRD pattern of the nanosheets after 15 minutes under the same condition revealing that they have been converted to magnetite.